Pharm Res (2012) 29:3455–3463
DOI 10.1007/s11095-012-0840-3

RESEARCH PAPER

Utilizing the Estrogen Receptor Ligand-Binding Domain for Controlled Protein Translocation to the Insoluble Fraction

James R. Davis • Mohanad Mossalam • Carol S. Lim

Received: 5 May 2012 / Accepted: 16 July 2012 / Published online: 7 August 2012

ABSTRACT

Purpose The estrogen receptor forms insoluble aggregates in the insoluble cytoskeletal subcellular fraction when bound to the antagonist fulvestrant. The ligand-binding domain was isolated and fused to signal sequences to target subcellular compartments. Sequestering a pro-apoptotic peptide tested the utility of a protein targeted to the insoluble fraction.

Methods The ligand-binding domain of the estrogen receptor was isolated and fused with signal sequences, either a nuclear localization signal or nuclear export signal. The subcellular localization when bound to drug fulvestrant was examined, specifically its interaction with cytokeratins 8 and 18. The ability to target a therapeutic peptide to the insoluble fraction was tested by fusing a therapeutic coiled-coil from Bcr-Abl in K562 cells.

Results The estrogen receptor ligand-binding domain responds to fulvestrant by translocating to the insoluble fraction. Adding a signal sequence significantly limited the translocation to either the nucleus or cytoplasm. The cytokeratin 8/18 status of the cell did not alter this response. The therapeutic coiled-coil fused to ERLBD was inactivated upon ligand induction.

Conclusions Isolating the ligand-binding domain of the estrogen receptor creates a ligand-controllable protein capable of translocation to the insoluble fraction. This can be used to sequester an active peptide to alter its function.

J. R. Davis • M. Mossalam • C. S. Lim
Department of Pharmaceutics and Pharmaceutical Chemistry
College of Pharmacy, University of Utah
Salt Lake City, Utah, USA

J. R. Davis
e-mail: james.r.davis@utah.edu

M. Mossalam
e-mail: mohanad.mossalam@utah.edu

C. S. Lim (✉)
421 Wakara Way, Rm. 318
Salt Lake City, Utah 84108, USA
e-mail: carol.lim@pharm.utah.edu

KEY WORDS cytokeratins · estrogen receptor · ligand binding domain · protein translocation · subcellular targeting

ABBREVIATIONS

CCmut3	mutated coiled-coil from Bcr-Abl
CK	cytokeratin
CP	cytoplasmic fraction
CS	cytoskeletal fraction
E2	estradiol
EGFP	enhanced green fluorescent protein
ER	estrogen receptor
ERLBD	estrogen receptor ligand binding domain
EtOH	ethanol
ICI	fulvestrant
LBD	ligand binding domain
NES	nuclear export signal
NLS	nuclear localization signal
OHT	4-hydroxytamoxifen
SERD	selective estrogen receptor downregulator
SERM	selective estrogen receptor modulator
SHR	steroid hormone receptor

INTRODUCTION

In nature, many proteins function exclusively in one subcellular compartment or another. Therefore, tight regulation of protein subcellular location provides a way for cells to control protein function in the complex cellular milieu. Much work in the past decade has focused on discovering, defining, and utilizing signal sequences for regulating protein location in cells (1,2). Subcloning allows the addition or removal of signal sequences to known proteins for altered location and function (1,3,4). For example, we have shown that it is now possible to send the normally oncogenic protein Bcr-Abl, the causative agent in chronic myelogenous

leukemia, to the nucleus, where it instead acts as an apoptotic factor (5). We also have shown that targeting p53 (a tumor suppressor) or c-Abl (a proto-oncogene) to the mitochondria can cause apoptosis (6,7). Our laboratory has also pioneered the concept of the "protein switch" where the location of a cytoplasmic protein can be made nuclear in a ligand-dependent fashion (3,4). We were also interested in creating different kinds of protein switches that would be capable of capturing active proteins and sequestering them into other subcellular compartments, rendering them inactive. This paper, to our knowledge, is the first to describe a protein switch capable of translocating from the nucleus or cytoplasm (or both) to an insoluble cytoskeletal fraction. This protein switch utilizes a version of the estrogen receptor ligand-binding domain (ERLBD) that is exclusively responsive to fulvestrant, a non-natural ligand that can be used for exquisite regulation of the protein location in the cell. We provide proof of concept of dysregulation of an active peptide (8) whose function is altered when triggered to the cytoskeletal fraction upon addition of ligand.

The ERLBD is derived from the estrogen receptor (ER), a member of the steroid hormone nuclear receptor (SHR) family (9). SHRs have an N-terminal activation domain, a central DNA binding domain, and a C-terminal ligand binding domain (LBD) (10). As with other steroid receptors, ER functions as a transcription factor when bound to its cognate agonist by dissociating from chaperone proteins and binding target DNA or other proteins involved in gene transcription (11,12). The stability of the ER has been shown to be dependent upon the ligand to which it is bound (13). In addition to activating gene transcription through the activation function domains, the endogenous ligand estradiol (E2) destabilizes ER levels by increasing proteasomal degradation and receptor turnover. The drug tamoxifen (one of the members of the selective estrogen receptor modulators, or SERMs) is a partial agonist at the ER, but also acts to stabilize the receptor. Fulvestrant (ICI 182,780, Faslodex®) is a member of the selective estrogen receptor down-regulators (SERDs) which act to disrupt the typical nucleocytoplasmic shuttling of ERα and result in cytoplasmic accumulation in a protein-synthesis dependent process (14,15). Fulvestrant is a clinically useful antiestrogen that prevents transcriptional activation and rapidly degrades ERα (13,14,16–22). The bulky side chain of fulvestrant induces a conformational change of helix 12 within ERα's LBD that increases hydrophobicity (23,24). Lupien *et al.* suggest receptor insolubility follows antagonist binding, mediated by hydrophobic residues L356, L540, and M543 residing in the helix 12 of the LBD (25). In HepG2 cells, the disappearance of the estrogen receptor after fulvestrant treatment appears to be caused by failure to extract the insoluble ER aggregates, though in MCF-7 cells receptor insolubility and degradation was observed. Long *et al.* speculate that the degradation of ER in the presence of fulvestrant is due to cytokeratins 8 and 18, which facilitate proteasomal degradation of ERα (19). Proteasomal degradation of ERα requires a functional helix 12 (19), and an active transcriptional activation complex (26–28). Removal of activation domains also prevents transactivation in the presence of receptor agonists, such as 17ß-estradiol. Cytokeratins 8 and 18 are the primary intermediate filaments of single-layer epithelial cells, and play a variety of roles including cell-cycle regulation, protection from cell stress and apoptosis (see Moll *et al.* and references within) (29). Unsurprisingly, these filaments may be useful in diagnostic immunohistochemistry, and may also be involved in the oncogensis of cutaneous squamous cell carcinoma (30), and may confer a favorable prognosis in breast carcinomas, likely due to the facilitation of ERα degradation in ER + tumors (19,31,32).

A GFP fusion protein with the ligand-binding domain of ER (ERLBD) was utilized to target the insoluble cytoskeletal fraction when bound to fulvestrant. The role of cytokeratins 8 and 18 in ERLBD cytoskeletal targeting is also examined. We show that fusing either a nuclear localization signal (NLS) or nuclear export signal (NES) to ERLBD can confer subcellular compartment specificity, thus allowing the ERLBD cytoskeleton interaction to occur either in the cytoplasm or nucleus. We also present an example of a protein capable of being sequestered in the insoluble fraction via the ERLBD, rendering it inactive.

MATERIALS AND METHODS

Cell Culture

The murine breast adenocarcinoma cell line 1471.1 (a kind gift from G. Hager, NCI, NIH) and human ovarian carcinoma cell line A2780 (Sigma Aldrich, St. Louis, MO) were grown as monolayers in DMEM (Invitrogen, Grand Island, NY) supplemented with 10% FBS (Invitrogen), 1% penicillin-streptomycin-L-glutamine (Invitrogen), 0.1% gentamicin (Invitrogen). Human breast adenocarcinoma MCF-7 cells (ATCC, Manassas, VA) were grown in monolayer in RPMI media (Invitrogen) supplemented as above, with the addition of insulin 4 mg/L (Sigma Aldrich). Monkey kidney fibroblast COS-7 cells were cultured as monolayer in RPMI media with antibiotic supplements. All cells were maintained in 5% CO_2 incubator at 37°C.

Plasmid Construction

A plasmid containing the ligand-binding domain of the human estrogen receptor α (amino acids 302 to 553, ERLBD) was a kind gift from Carolyn Smith (Baylor

College of Medicine). To subclone ERLBD into the multiple cloning site (MCS) of EGFP-C1, a KpnI restriction site was introduced before the ERLBD by site-directed mutagenesis with top primer 5'-GGACAAGGCCAGGCTG TTCTTCTTAGAGGTACCAC-CGGATCTAGATAAC TGATC-3' and bottom primer 5'-GATCAGTTATCTA GATCCGGTGGTACCTCTAAGAAGAACAGCCT GGCCTTGTCC-3'. The KpnI digested ERLBD fragment was subcloned into the KpnI site of EGFP-C1 resulting in EGFP-ERLBD. Sequence analysis (at the University of Utah Core DNA Sequencing Facility) verified successful cloning.

To create EGFP-NLS-ERLBD, the NLS sequence from SV40 large T-antigen was placed between BspEI and XhoI sites. The oligonucleotides containing the NLS sequence were synthesized by the core facility, and were annealed together, creating a double stranded insert flanked by BspEI and XhoI overhangs. The sequences for the oligonucleotides are as follows: top strand: 5'-CCGGAAGCCCGAAAA AAAAACGCAAAGTGGAATC-3' and bottom strand: 5' TCGAGATTCCACTTTGCGTTTTTTTTTCGG GCTT-3'. The annealed oligonucleotides were ligated into a digested EGFP-ERLBD vector. Similarly, the NES from mitogen activated protein kinase kinase (MAPKK) was cloned between BspE1 and XhoI to form EGFP-NES-ERLBD. The oligos were synthesized as follows: top strand: 5'-CCGGACTGCAGAAAAAACTGGAAGAACTG GAACTGTC-3' and bottom strand: 5'-TCGAGA CAGTTCCAGTTCTTCCAGTTTTTTCTGCAGT-3'. In addition, the EGFP-ERLBD-CCmut3 was constructed by amplifying the DNA encoding ERLBD by polymerase chain reaction, using the primers 5′-GGATCACTCTC GGCATGG-3′ and 5′-GCGCGCGCGCTCCGGAGCTA GTGGGCGCATGTAGG-3′ followed with BspEI digestion. This was subcloned into the BspEI restriction enzyme site in our published EGFP-CCmut3 plasmid (8).

Transient Transfections

For microscopy studies, cells were plated on a clear cover glass in six well plates (Greiner Bio-One Cellstar, Monroe, NC) or live cell chambers (Nalg Nunc, Rochester, NY) with corresponding media the day before transfection. For western blot, cells were plated in 60 mm dishes (Corning Inc., Corning, NY). Transfections were performed with Lipofectamine 2000 (Invitrogen) per manufacturer's recommendations. K562 cells were transfected according to the Cell Line Nucleofector Kit V Protocol (program T-013) using the Amaxa Nucleofector II (Lonza Group, Basel, Switzerland).

Microscopy and Image Analysis

Approximately 16 to 24 h after transfection, cells were viewed on an Olympus IX701F inverted fluorescence microscope (Scientific Instrument Company, Aurora, CO) as previously described (33). To quantitate protein location, the fluorescent images obtained were analyzed using analySIS® software (Soft Imaging System, Lakewood, CO) as previously described (4). To obtain average cytoplasmic intensity data for all constructs, 10 representative cells from each experiment were analyzed and averaged from 3 separate experiments (n=3), and are expressed as percent cytoplasmic intensity. Statistical differences between the constructs were determined using one-way ANOVA with Tukey's post-hoc test.

Western Blot

Approximately 24 h after transfection, cells were treated as indicated, briefly rinsed with PBS, removed from the dish by trypsinization, then centrifuged at 500 × g for 5 min. Cell lysis and subcellular fractionation were carried out with the Subcellular Protein Fractionation Kit (Thermo Scientific). Cytoplasmic and cytoskeletal fractions were separated on a Novex Bis-Tris 10% gel (Invitrogen), transferred to PVDF membrane by iBlot (Invitrogen). Blocking was accomplished with Blocker BLOTTO (Thermo Scientific, Rockford, IL). Primary antibodies were diluted in Blocker BSA 2% (Thermo Scientific) in TBST. For detection of cytokeratin 18, a rabbit polyclonal to cytokeratin 18 (Abcam ab52948, Cambridge, MA) was used, diluted to 1:10,000. For detection of GFP, rabbit polyclonal Anti-GFP (Sigma Aldrich G1544) was diluted to 1 µl/mL. Loading control anti-GAPDH (Cell Signaling #5174, Danvers, MA) was diluted to 1:1000. Secondary anti-rabbit IgG conjugated to horseradish peroxidase (Cell Signaling #7074) was diluted 1:2500 in BSA 2% in TBST. To produce chemiluminescence, the SuperSignal West Pico Chemiluminescent substrate (Thermo Scientific) was incubated on the membrane. Western images were acquired with FluorChem FC2 imaging station with AlphaView Software (AlphaInnotech, San Leandro, CA).

Indirect Immunofluorescence

Approximately 24 h after transfection, MCF-7 cells were treated with drug or vehicle for 1 h, and then rinsed briefly with ice-cold PBS. Cells were fixed with 4% paraformaldehyde solution for 15 min at room temperature, and then washed twice with ice-cold PBS. Cell membranes were permeabilized with 0.5% Triton X-100 in PBS for 10 min, and then washed with PBS three times for 5 min each. Blocking was done with BLOTTO for 1 h. Primary antibody against CK18 was diluted 1:500 in 5% BSA in PBS, and then incubated with cells for 1 h at room temperature. Cells were washed x 3 with PBS for five minutes. Goat anti-rabbit secondary antibody conjugated to Texas Red (Abcam

ab6719) was diluted 1:500 in BLOTTO and incubated with cells for 1 h at room temperature. Excess antibody was removed by washing x 3 for 5 min. Cover slips were mounted to glass slides with Fluoromount G (Electron Microscopy Sciences, Hatfield, PA). Fixed slides were viewed with an Olympus IX81 FV1000-XY confocal microscope (Imaging Core Facility, University of Utah) with a 60X objective and 3.0x digital zoom as previously described (8). Excitation and emission filters for EGFP and Texas Red were 488 nm excitation, 500–530 nm emission filter, and 543 excitation, 555–655 nm emission filter, respectively. To account for variations in expression of EGFP, the exposure settings and laser gain of each channel were kept below detected pixel saturation for each cell. Olympus FluoView software was used to capture images; ImageJ (http://rsb.info.nih.gov/ij) was used for image analysis. Prior to statistical analysis, cell images were corrected for background noise. Identical regions of interest (ROIs) were created around whole cells for each fluorophore, and these ROIs were compared using JACoP colocalization plugin to estimate Costes' colocalization coefficient (34,35). To better visualize colocalization, the Colocalization ColorMap plugin was used (36).

7AAD Assay

K562 cells were stained with 7-aminoactinomycin D (7-AAD, Invitrogen) according to manufacturer's instructions 48 and 72 h after transfection. The samples were analyzed using the FACSCanto-II (BD-BioSciences, University of Utah Core Facility) with FACSDiva software. Only transfected cells were analyzed by gating for EGFP positive cells. EGFP and 7-AAD were excited with the 488 nm laser, and were detected at 507 nm and 660 nm, respectively. Each construct was assayed three times (n=3). The means of each group were compared by ANOVA with Tukey's post-hoc test.

RESULTS

Subcellular Localization

Three protein constructs were constructed and transiently transfected into various cell lines. Figure 1 shows the results from microscopy of these cells. The first construct tested was EGFP-ERLBD, a truncation of the human ERα consisting of amino-acids 302–595. This region of the receptor is responsible for ligand binding and transactivation, but lacks the domains capable of interacting with DNA. The result is a construct that takes on whole-cell localization when viewed by fluorescence microscopy in the presence of ethanol (vehicle), but in the presence of fulvestrant takes on a punctate staining pattern. The basal localization is in contrast to full-length receptor that localizes exclusively in the nucleus, and only appears in the cytoplasm after fulvestrant addition (14). This distribution was visualized in murine breast adenocarcinoma cell line 1471.1, human breast adenocarcinoma MCF-7 cells, human cervical carcinoma HeLa cells, and monkey kidney fibroblast COS-7 cells.

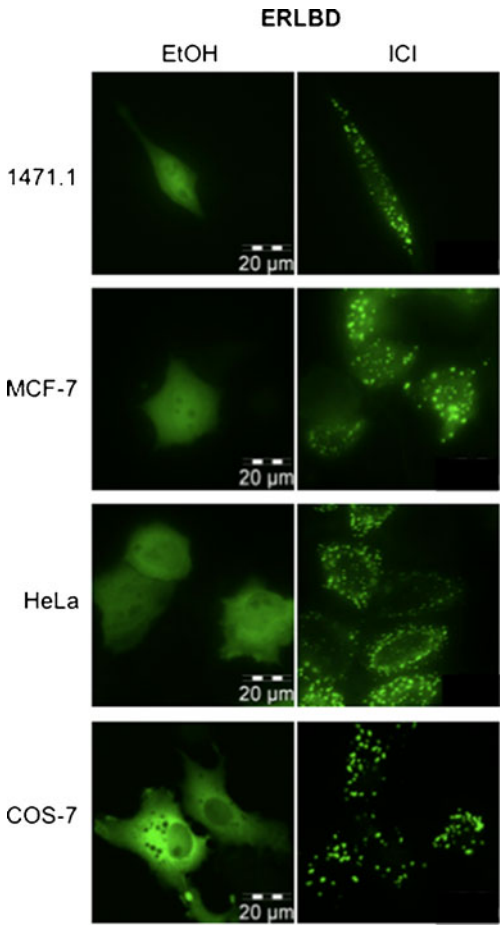

Fig. 1 Representative fluorescence microscopy images of cells from multiple cell types (1471.1, MCF-7, HeLa, or COS-7 cells) transfected with EGFP-ERLBD. Cells were treated with EtOH (ethanol, left) or fulvestrant (ICI, right) 100 nM for 1 h. With EtOH treatment, the protein can be seen as having a whole-cell distribution. When treated with fulvestrant, the protein was seen in dense punctate clusters, in both the cytoplasm and nucleus.

To test the ability to control the subcellular localization of the construct in these cell lines, we then fused a nuclear export signal from the mitogen activating protein kinase kinase (MAPKK) "NES-ERLBD", or a classical monopartite nuclear localization signal from the SV40 large-T antigen "NLS-ERLBD" (Fig. 2). The results demonstrate an ability to predetermine the subcellular compartment of an introduced protein. The NES excludes the introduced protein from the nucleus (Fig. 2, left half), with or without the presence of fulvestrant, and the NLS robustly directs the protein into the nucleus (Fig. 2, right half).

Quantification of the amount of fluorescence of each construct in the cytoplasm in 1471.1 cells was done

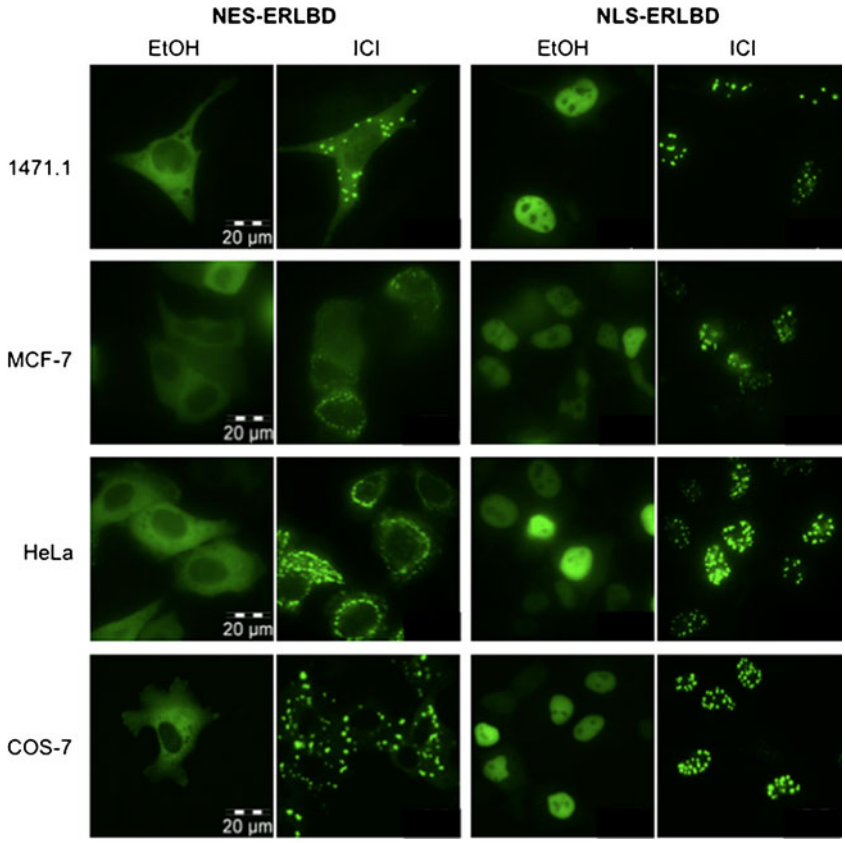

Fig. 2 The inclusion of signals sequences changes the distribution of ERLBD across multiple cell types (1471.1, MCF-7, HeLa, or COS-7 cells). A nuclear export signal fused to EGFP-ERLBD (left) shows a more prominent cytoplasmic distribution with or without treatment with fulvestrant 100 nM for 1 h. A nuclear localization signal (right) clearly demonstrates a pronounced nuclear accumulation with or without fulvestrant. In both cases, a change to punctate clusters occurs in the presence of fulvestrant in their respective subcellular compartment (nucleus or cytoplasm).

(Fig. 3a). ERLBD was found to have 36.7%±2.2 cytoplasmic fluorescence, NES-ERLBD had 54.5%±1.5, and NLS-ERLBD had 20.9%±2.7. Compared to ERLBD, NES and NLS constructs were significantly different, with p-value < 0.001. Figure 3b shows the fluorescence from a region within the cell before and after drug addition, demonstrating the displacement of proteins to aggregates. Figure 3c shows the change, in percent, of this movement. The negative value signifies the loss of fluorescence in a defined region of interest as the protein translocates away from the region to insoluble punctate dots. Only ERLBD and NLS-ERLBD showed high protein displacement after fulvestrant addition (>80%). Nevertheless, NES-ERLBD does show a change in the cytoplasmic pattern, going from a dispersed to a punctate pattern, but no overall displacement of fluorescence intensity in that region.

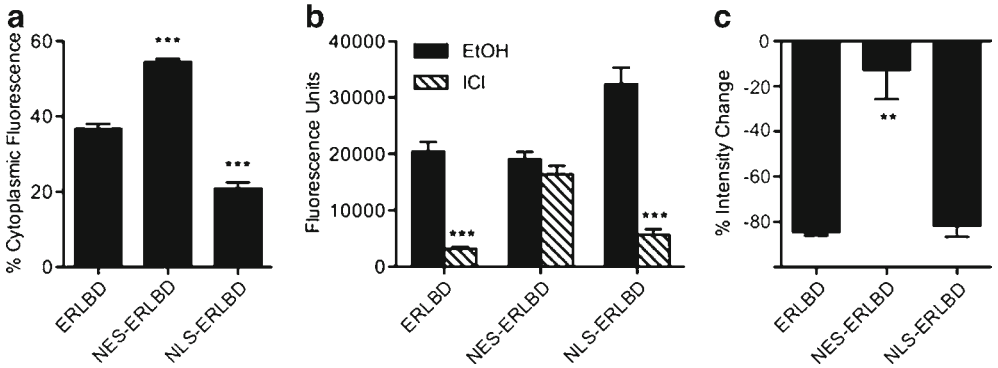

Fig. 3 Fluorescence intensity analysis in the cytoplasmic and nuclear compartment of 1471.1 cells. (**a**) Fusion of an NES (NES-ERLBD) significantly increased ($p < 0.001$) the fluorescence intensity in the cytoplasm compared to ERLBD. The fusion of an NLS (NLS-ERLBD) significantly decreased the fluorescence intensity in the cytoplasm (meaning an increase in nuclear intensity) compared to ERLBD, $p < 0.001$. (**b**) Quantitation of fluorescence intensity displacement when treated with fulvestrant 100 nM for 1 h. ERLBD and NLS-ERLBD showed significant displacement when bound to fulvestrant compared to EtOH treatment, $p < 0.001$. NES-ERLBD did not show significant displacement, $p > 0.05$. (**c**) Percent change of fluorescence intensity after fulvestrant addition (negative values represent loss of fluorescence in defined region of interest). The response to fulvestrant was robust in ERLBD and NLS-ERLBD transfected cells, with a high intensity change of greater than 80%. The response by NES-ERLBD to drug was significantly lower compared to ERLBD and NLS-ERLBD, $p < 0.01$. ***=$p < 0.001$, **=$p < 0.01$.

ERLBD Localization by Fractionation

It has been proposed that the distribution change of ER when bound to fulvestrant is due to an interaction with cytoskeletal cytokeratins (19). To examine this possible interaction, microscopy and subcellular fractionation of a cytokeratin-negative cell line A2780 was compared to cytokeratin positive MCF-7 cells. Microscopy of A2780 (Fig. 4a) reveals the same pattern of cytoplasm-to-punctate pattern seen in other cell lines transfected with EGFP-ERLBD in the presence of fulvestrant. Subcellular fractionation of untransfected (naked DNA only) *versus* transfected was performed to rule-out possible upregulation of cytokeratins by Lipofectamine reagent alone (Fig. 4b). Lipofectamine transfection did not result in any upregulation of CKs 8/18 in cytoplasmic (CP) or cytoskeletal (CS) fractions (Fig. 4b, "Lipo +/−). MCF-7 cells are known to be cytokeratin positive, and these cells did demonstrate cytokeratins in both untransfected and transfected cells. Knowing the cytokeratin status of these cells, the subcellular fraction of EGFP-ERLBD was evaluated 1 h after ethanol (ICI -) or fulvestrant 100 nM (ICI +) treatment conditions (Fig. 4c). In both A2780 and MCF-7 cells, EGFP-ERLBD resided in the cytoplasm (Fig. 4c, CP, -) when induced with vehicle. However, fulvestrant induced a change in subcellular location to the cytoskeleton (Fig. 4c, CS, +). Hence we conclude that the cytokeratin status does not affect the subcellular location of EGFP-ERLBD bound to fulvestrant.

Cytokeratin 18/ERLBD Colocalization

To further assess the interaction of the ERLBD truncation with cytokeratins, indirect immunofluorescence of CK18 (red channel) on fixed MCF-7 cells transiently transfected with ERLBD (green channel) was performed. A single plane of each cell was captured in both red and green channels (Fig. 5). The distribution of ERLBD was similar to that seen in Fig. 1, with whole-cell distribution after ethanol treatment, and punctate distribution after fulvestrant treatment Fig. 5a, top and bottom panels). CK18 as visualized by indirect immunofluorescence revealed a typical cytoskeletal interconnected filament pattern (Fig. 5b, top and bottom panels). The images were pseudocolored with red or green, and merged to visualize colocalization. The merged images revealed little yellow color—which denotes overlapping fluorescence in the red and green channels, so a Colocalization Colormap plugin was utilized in ImageJ to better visualize truly overlapping pixels, and JACoP plugin was used to quantify the colocalization by the Costes' coefficient, which quantifies the colocalization of two fluorophores by statistically correlating the overlap and pixel intensity of each color (35). The Costes' coefficient predicts colocalized fluorophores for values over 0.5. High degrees of pixel intensity overlap are depicted in the colormap by red and brown colors, where low degrees of overlap are depicted as blue and green (Fig. 5d, top and bottom panels). ERLBD treated with ethanol had a Costes' coefficient of 0.38 ± 0.05; whereas with fulvestrant treatment yielded a coefficient of 0.089 ± 0.03. Neither treatment condition suggests a significant colocalization of the ERLBD with cytokeratin 18.

Induced Sequestration of ERLBD-Bearing Protein

To test the ability of ERLBD to control a protein's localization, and therefore function, we subcloned a mutated coiled-coil (CCmut3) motif from Bcr-Abl previously developed in our lab (8). When introduced into Bcr-Abl positive CML cells, this coiled-coil disrupts signaling by Bcr-Abl and

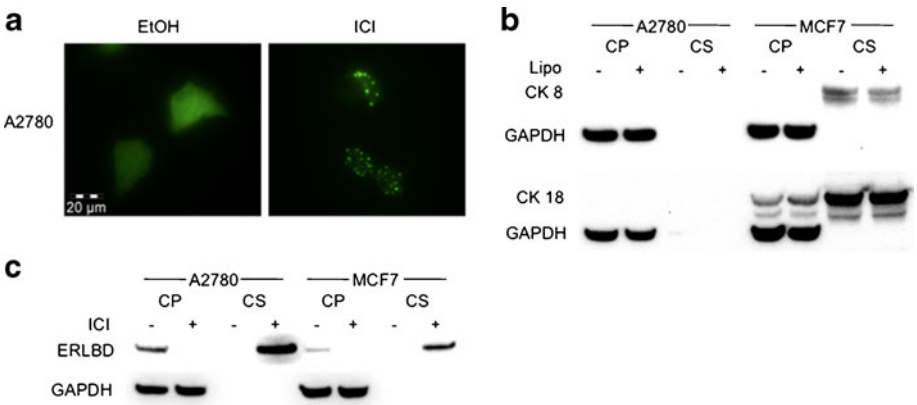

Fig. 4 (**a**) Fluorescence microscopy images of A2780 cells transfected with EGFP-ERLBD, and treated with EtOH or fulvestrant 100 nM for 1 h. (**b**) Western blot after subcellular fractionation of A2780 and MCF-7 cells, with (+) or without (−) transfection by lipofection. Cytokeratins (CK) 8 and 18 were only detected in MCF-7 cells, regardless of transfection status, and appeared only in the cytoskeletal fraction (CS), not the cytoplasmic fraction (CP) while no CK8 or CK18 were detected in A2780. GAPDH was used as a marker of cytoplasmic proteins. (**c**) ERLBD was detected in the cytoplasmic fraction (CP) when treated with ethanol (−), but was seen exclusively in the cytoskeletal fraction (CS) after fulvestrant treatment (+). This response was visible in both A2780 and MCF-7 cells.

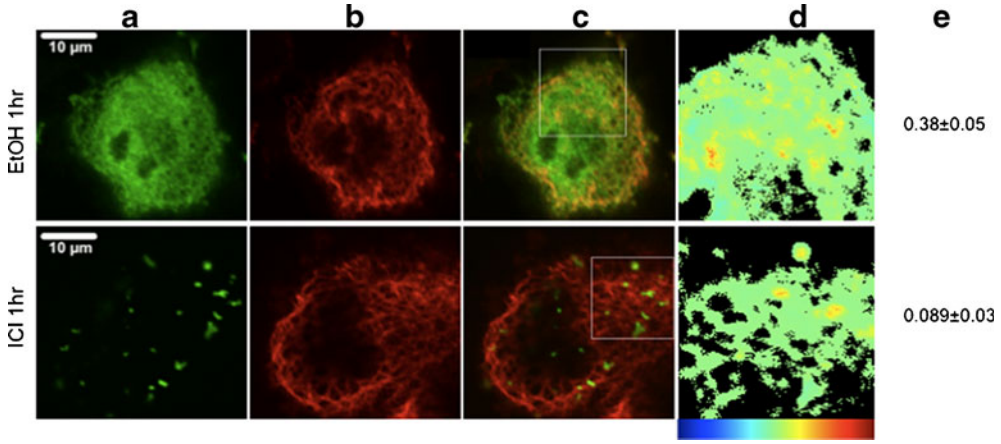

Fig. 5 Indirect immunofluorescence confocal microscopy images of MCF-7 cells transfected with EGFP-ERLBD, stained with anti-cytokeratin 18. (**a**) Location of EGFP-ERLBD with ethanol or fulvestrant treatment. (**b**) Cytokeratin 18 in both treatment conditions. (**c**) Merged image of both green and red channels. Overlapping red and green pixels appear as yellow. (**d**) Expanded region from (**c**), depicted as a colocalization heatmap, with high degrees of pixel color and intensity overlap as dark red, low degrees as blue. (**e**) Pearson's corrected Costes' Coefficient, a quantitation of protein colocalization by JACoP plugin (ImageJ). Significantly colocalized proteins have coefficients greater than 0.5. Significant colocalization was not seen with ethanol or fulvestrant treatment.

induces apoptosis. We hypothesized that ERLBD-CCmut3, when bound to fulvestrant, would cause sequestration of CCmut3 thereby preventing the disruption of Bcr-Abl signaling and nullifying its apoptotic response. Microscopy studies reveal that fulvestrant does indeed sequester ERLBD-CCmut3 similarly to ERLBD alone in K562 cells, whereas ER agonist estradiol and partial agonist tamoxifen did not induce protein translocation (Fig. 6a). To test the decrease in

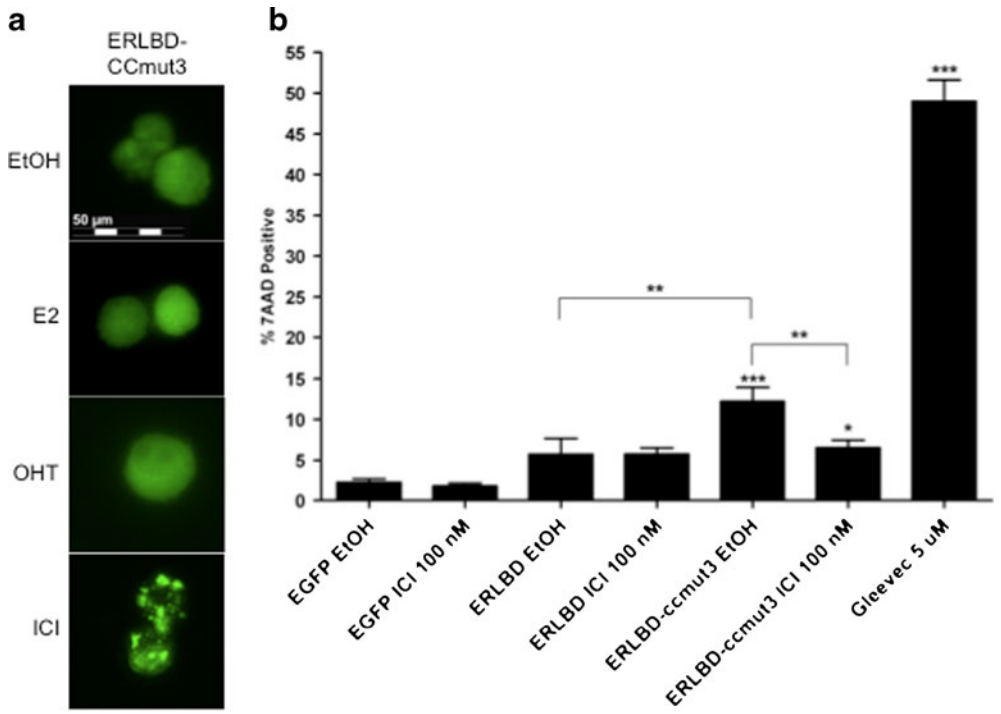

Fig. 6 (**a**) Fluorescence microscopy of K562 cells transfected with EGFP-ERLBD-CCmut3 and treated with either ethanol (EtOH), estradiol (E2) 100 nM, tamoxifen (OHT) 100nM, or fulvestrant (ICI) 100nM for 1 h. Fulvestrant was the only ligand causing appreciable protein translocation. The same subcellular distribution pattern was demonstrated when treated with fulvestrant, despite the inclusion of a functional peptide capable of binding an endogenous protein. (**b**) 7AAD staining as detected by flow cytometry, as a percent of cell population. Only cells transfected with ERLBD-CCmut3 showed significantly higher 7AAD staining than the negative control (EGFP). ERLBD-CCmut3 treated with ethanol demonstrated the highest staining of transfected cells, significantly higher than EGFP, $p < 0.001$. When bound to fulvestrant, however, 7AAD staining significantly decreased, $p < 0.01$. Untransfected cells were treated with Gleevec® as a positive control for 7AAD staining. ***=$p < 0.001$, **=$p < 0.01$, *$p < 0.05$

apoptotic potential of ERLBD-CCmut3 sequestered by fulvestrant, flow cytometry with 7AAD staining was performed. Bcr-Abl positive K562 CML cells were transfected with EGFP, EGFP-ERLBD, or EGFP-ERLBD-CCmut3. These cells were treated with ethanol or fulvestrant at escalating doses for 48 and 72 h; untransfected cells were treated with Gleevec® as a positive control (Fig. 6b). EGFP with or without fulvestrant demonstrated low 7AAD staining, with 2.2%±0.4 and 1.8%±0.4 respectively. EGFP-ERLBD trended toward higher 7AAD staining, though not statistically significant with either ethanol or fulvestrant treatment: 5.7%±1.9, and 5.7% ±0.8, respectively. The construct with CCmut3 significantly increased 7AAD staining compared to EGFP as expected due to disruption of Bcr-Abl signaling, but only when treated with ethanol (vehicle), 12.2%±1.7, $p<0.001$. When treated with fulvestrant, the sequestration of CCmut3 allowed Bcr-Abl to continue its proliferative effects, with decreased apoptosis as measured by 7AAD to 5.8%±0.8 (significantly different from ethanol treatment, $p<0.01$). The results were consistent at 48 (data not shown) and 72 h of treatment. Fulvestrant was also tested at higher doses (400 nM and 800 nM), though these were not significantly different from 100 nM (data not shown).

DISCUSSION

Our lab has previously had success in creating novel "protein switches" capable of ligand-dependent subcellular translocation of exogenous proteins. To our knowledge, this is the first paper to describe harnessing the ligand-inducible translocation of the estrogen receptor ligand-binding domain (ERLBD) to generate a protein switch capable of controlled movement from the cytoplasm, and/or nucleus to the insoluble cytoskeletal fraction. This controlled translocation is accomplished when the LBD binds the synthetic antagonist fulvestrant. The estrogen receptor (ER) is a protein that typically resides in the nucleus, but when bound to the SERD fulvestrant, is found in insoluble clusters in both the nucleus and cytoplasm (14,15). Here, we showed that removing the ligand-binding domain (LBD) from the full-length receptor still responds to fulvestrant, but that its localization can be controlled by the lack-of or inclusion-of signal sequences. Microscopy studies revealed that the inclusion of a nuclear localization signal (NLS) directed the protein to the nucleus before ligand, and maintained the nuclear location while forming insoluble aggregates upon ligand addition. Similarly, fusing a nuclear export signal (NES) to the LBD directed the protein to the cytoplasm. This control of protein localization was demonstrated in a wide array of cell types, including those with or without cytokeratins 8 and 18, and cancer or non-cancer types. Previously, the response of the ER to fulvestrant was attributed to its interaction with cytokeratins 8 and 18 in both the cytoplasm and the nucleus (19), and this was also claimed to be an intermediate step toward proteasomal degradation when bound to ligand (13,19). Our subcellular fractionation in MCF-7 cells (cytokeratin 8 and 18 positive) *and* A2780 (cytokeratin 8 and 18 negative) showed that the ERLBD fusion protein is capable of translocation from the cytoplasm to the insoluble cytoskeletal fraction regardless of cytokeratin status. Confocal microscopy confirmed that colocalization of ERLBD with cytokeratins was minimal, and played no role. Perhaps in other studies, localization to CK 8 and 18 may be mediated by other domains of the ER not present in our ERLBD constructs.

The utility of this controlled localization was demonstrated by fusing the ERLBD protein to a functional peptide (CCmut3) that had previously been shown to bind to and disrupt Bcr-Abl signaling in K562 cells and induce apoptosis (8). We hypothesized that after fulvestrant addition, ERLBD-CCmut3 protein would translocate away from Bcr-Abl to insoluble clusters, and would relieve the Bcr-Abl signaling inhibition. Indeed, despite the fact that CCmut3 interacts with Bcr-Abl, microscopy studies corroborated that ERLBD-CCmut3 formed insoluble clusters with the addition of fulvestrant, indicating ligand-inducible controlled localization of CCmut3. Lastly, ERLBD-CCmut3 showed apoptosis without fulvestrant, but a significant drop in apoptosis when bound to drug, confirming our hypothesis of location altering function. This technology has the potential to be used as a controlled tool to test and verify synthetic exogenous protein or peptide function, as demonstrated here, but may also be useful to induce an *in trans* sequestration of an endogenous protein target. Any protein binding domain can easily be cloned into an ERLBD vector, thus allowing a large variety of potential cellular targets, in multiple cell types.

ACKNOWLEDGMENTS AND DISCLOSURES

This work was funded in part by DOD Breast Cancer Concept Award DOD 55900381, NIH RO1-CA129528, NIH R01-CA129528, and NIH R01-CA151847. JRD would like to thank the American Foundation for Pharmaceutical Education (AFPE) for support. We acknowledge the use of the DNA/Peptide Core (NCI Cancer Center Support Grant P30 CA042014, Huntsman Cancer Institute). We would like to thank Andrew Dixon, David Woessner, Jonathan Constance, Karina Matissek, Benjamin Bruno, Abood Okal, Geoffrey Miller, and Shams Reaz for scientific discussions. The authors declare no conflict of interest or disclosures.

REFERENCES

1. Davis JR, Kakar M, Lim CS. Controlling protein compartmentalization to overcome disease. Pharm Res. 2007;24(1):17–27. Epub 2006/09/14.

2. Mossalam M, Dixon AS, Lim CS. Controlling subcellular delivery to optimize therapeutic effect. Ther Deliv. 2010;1(1):169–93. Epub 2010/11/30.
3. Kakar M, Cadwallader AB, Davis JR, Lim CS. Signal sequences for targeting of gene therapy products to subcellular compartments: the role of CRM1 in nucleocytoplasmic shuttling of the protein switch. Pharm Res. 2007;24(11):2146–55. Epub 2007/06/15.
4. Kakar M, Davis JR, Kern SE, Lim CS. Optimizing the protein switch: altering nuclear import and export signals, and ligand binding domain. J Control Release. 2007;120(3):220–32. Epub 2007/06/19.
5. Dixon AS, Kakar M, Schneider KM, Constance JE, Paullin BC, Lim CS. Controlling subcellular localization to alter function: sending oncogenic Bcr-Abl to the nucleus causes apoptosis. J Control Release. 2009;140(3):245–9. Epub 2009/07/07.
6. Mossalam M, Matissek KJ, Okal A, Constance JE, Lim CS. Direct induction of apoptosis using an optimal mitochondrially targeted p53. Mol Pharm. 2012. Epub 2012/03/03.
7. Constance JE, Despres SD, Nishida A, Lim CS. Selective targeting of c-Abl via a cryptic mitochondrial targeting signal activated by cellular redox status in leukemic and breast cancer cells. Pharm Res. 2012;In Press.
8. Dixon AS, Miller GD, Bruno BJ, Constance JE, Woessner DW, Fidler TP, *et al.* Improved coiled-coil design enhances interaction with Bcr-Abl and induces apoptosis. Mol Pharm. 2012;9(1):187–95. Epub 2011/12/06.
9. Evans RM. The steroid and thyroid hormone receptor superfamily. Science. 1988;240(4854):889–95. Epub 1988/05/13.
10. Tsai MJ, O'Malley BW. Molecular mechanisms of action of steroid/thyroid receptor superfamily members. Annu Rev Biochem. 1994;63:451–86. Epub 1994/01/01.
11. Beato M, Herrlich P, Schutz G. Steroid hormone receptors: many actors in search of a plot. Cell. 1995;83(6):851–7. Epub 1995/12/15.
12. Brzozowski AM, Pike AC, Dauter Z, Hubbard RE, Bonn T, Engstrom O, *et al.* Molecular basis of agonism and antagonism in the oestrogen receptor. Nature. 1997;389(6652):753–8. Epub 1997/10/24 21:29.
13. Preisler-Mashek MT, Solodin N, Stark BL, Tyriver MK, Alarid ET. Ligand-specific regulation of proteasome-mediated proteolysis of estrogen receptor-alpha. Am J Physiol Endocrinol Metab. 2002;282(4):E891–8. Epub 2002/03/08.
14. Dauvois S, White R, Parker MG. The antiestrogen ICI 182780 disrupts estrogen receptor nucleocytoplasmic shuttling. J Cell Sci. 1993;106(Pt 4):1377–88. Epub 1993/12/01.
15. Htun H, Holth LT, Walker D, Davie JR, Hager GL. Direct visualization of the human estrogen receptor alpha reveals a role for ligand in the nuclear distribution of the receptor. Mol Biol Cell. 1999;10(2):471–86. Epub 1999/02/09.
16. Alarid ET, Bakopoulos N, Solodin N. Proteasome-mediated proteolysis of estrogen receptor: a novel component in autologous down-regulation. Mol Endocrinol. 1999;13(9):1522–34. Epub 1999/09/09.
17. Eckert RL, Mullick A, Rorke EA, Katzenellenbogen BS. Estrogen receptor synthesis and turnover in MCF-7 breast cancer cells measured by a density shift technique. Endocrinology. 1984;114(2):629–37. Epub 1984/02/01.
18. Stenoien DL, Patel K, Mancini MG, Dutertre M, Smith CL, O'Malley BW, *et al.* FRAP reveals that mobility of oestrogen receptor-alpha is ligand- and proteasome-dependent. Nat Cell Biol. 2001;3(1):15–23. Epub 2001/01/09.
19. Long X, Nephew KP. Fulvestrant (ICI 182,780)-dependent interacting proteins mediate immobilization and degradation of estrogen receptor-alpha. J Biol Chem. 2006;281(14):9607–15. Epub 2006/02/07.
20. McDonnell DP. The molecular pharmacology of estrogen receptor modulators: implications for the treatment of breast cancer. Clin Cancer Res. 2005;11(2 Pt 2):871s–7s. Epub 2005/02/11.
21. MacGregor JI, Jordan VC. Basic guide to the mechanisms of antiestrogen action. Pharmacol Rev. 1998;50(2):151–96. Epub 1998/07/02.
22. Wijayaratne AL, McDonnell DP. The human estrogen receptor-alpha is a ubiquitinated protein whose stability is affected differentially by agonists, antagonists, and selective estrogen receptor modulators. J Biol Chem. 2001;276(38):35684–92. Epub 2001/07/27.
23. Wu YL, Yang X, Ren Z, McDonnell DP, Norris JD, Willson TM, *et al.* Structural basis for an unexpected mode of SERM-mediated ER antagonism. Mol Cell. 2005;18(4):413–24. Epub 2005/05/17.
24. Pike AC, Brzozowski AM, Walton J, Hubbard RE, Thorsell AG, Li YL, *et al.* Structural insights into the mode of action of a pure antiestrogen. Structure. 2001;9(2):145–53. Epub 2001/03/16.
25. Lupien M, Jeyakumar M, Hebert E, Hilmi K, Cotnoir-White D, Loch C, *et al.* Raloxifene and ICI182,780 increase estrogen receptor-alpha association with a nuclear compartment via overlapping sets of hydrophobic amino acids in activation function 2 helix 12. Mol Endocrinol. 2007;21(4):797–816. Epub 2007/02/15.
26. Arnold SF, Obourn JD, Jaffe H, Notides AC. Serine 167 is the major estradiol-induced phosphorylation site on the human estrogen receptor. Mol Endocrinol. 1994;8(9):1208–14. Epub 1994/09/01.
27. Castano E, Vorojeikina DP, Notides AC. Phosphorylation of serine-167 on the human oestrogen receptor is important for oestrogen response element binding and transcriptional activation. Biochem J. 1997;326(Pt 1):149–57. Epub 1997/08/15.
28. Valley CC, Metivier R, Solodin NM, Fowler AM, Mashek MT, Hill L, *et al.* Differential regulation of estrogen-inducible proteolysis and transcription by the estrogen receptor alpha N terminus. Mol Cell Biol. 2005;25(13):5417–28. Epub 2005/06/21.
29. Moll R, Divo M, Langbein L. The human keratins: biology and pathology. Histochem Cell Biol. 2008;129(6):705–33. Epub 2008/05/08.
30. Yamashiro Y, Takei K, Umikawa M, Asato T, Oshiro M, Uechi Y, *et al.* Ectopic coexpression of keratin 8 and 18 promotes invasion of transformed keratinocytes and is induced in patients with cutaneous squamous cell carcinoma. Biochem Biophys Res Commun. 2010;399(3):365–72. Epub 2010/07/28.
31. Long X, Fan M, Nephew KP. Estrogen receptor-alpha-interacting cytokeratins potentiate the antiestrogenic activity of fulvestrant. Cancer Biol Ther. 2010;9(5):389–96. Epub 2010/01/12.
32. Woelfle U, Sauter G, Santjer S, Brakenhoff R, Pantel K. Down-regulated expression of cytokeratin 18 promotes progression of human breast cancer. Clin Cancer Res. 2004;10(8):2670–4. Epub 2004/04/23.
33. Dixon AS, Lim CS. The nuclear translocation assay for intracellular protein-protein interactions and its application to the Bcr coiled-coil domain. Biotechniques. 2010;49(1):519–24. Epub 2010/07/10.
34. Bolte S, Cordelieres FP. A guided tour into subcellular colocalization analysis in light microscopy. J Microsc. 2006;224(Pt 3):213–32. Epub 2007/01/11.
35. Costes SV, Daelemans D, Cho EH, Dobbin Z, Pavlakis G, Lockett S. Automatic and quantitative measurement of protein-protein colocalization in live cells. Biophys J. 2004;86(6):3993–4003. Epub 2004/06/11.
36. Jaskolski F, Mulle C, Manzoni OJ. An automated method to quantify and visualize colocalized fluorescent signals. J Neurosci Methods. 2005;146(1):42–9. Epub 2005/06/07.